AIP Applied Physics Letters

# Band-gap narrowing in ordered and disordered semiconductor alloys

S.-H. Wei and Alex Zunger

Citation: Applied Physics Letters **56**, 662 (1990); doi: 10.1063/1.103307
View online: http://dx.doi.org/10.1063/1.103307
View Table of Contents: http://scitation.aip.org/content/aip/journal/apl/56/7?ver=pdfcov
Published by the AIP Publishing

# Band-gap narrowing in ordered and disordered semiconductor alloys

S.-H. Wei and Alex Zunger
*Solar Energy Research Institute, Golden, Colorado 80401*

(Received 13 October 1989; accepted for publication 4 December 1989)

Either spontaneous or artificial ordering of semiconductor alloys into CuAu-like, chalcopyrite, or CuPt-like structures is predicted to be accompanied by a reduction in the direct band gaps relative to the average over the binaries. In this letter calculated results are presented for seven III-V and II-VI alloys. We identify the mechanism for this band-gap narrowing as band folding followed by repulsion between the folded states. The latter is coupled by the non-zinc-blende component of the superlattice potential. The same physical mechanism (but to a different extent) is responsible for gap bowing in *disordered* alloys.

Recent theoretical predictions[1,2] and experimental observations[3-6] demonstrated that isovalent pseudobinary $A_{1-x}B_xC$ semiconductor alloys can order into CuAu-like (CA),[3] chalcopyrite (CH),[4] and CuPt-like[5,6] (CP) structures. We have calculated the band gaps of seven alloys in each of these three structures, as well as those of the disordered alloys at the same 50–50% composition. We find ordering-induced band-gap narrowing with respect to the linearly averaged gaps of the binary constituents, and analyze the physical origins for these variations.

We calculated self-consistently the relativistic band structures of $AlGaAs_2$, $CdZnTe_2$, $GaInP_2$, $HgZnTe_2$, $CdHgTe_2$, $GaInAs_2$, and $Ga_2AsSb$, using the local density approximation as implemented by the linearized augmented plane wave (LAPW) method.[7] In each case, we first optimize the crystal structure to reach a minimum in the total energy. This includes both cell-external (i.e., lattice) parameters and cell-internal (i.e., atomic positions inside the unit cells whose value is not fixed by symmetry) parameters. Details of the method are given in Ref. 2. The 50–50% disordered alloy is represented by the "special quasirandom structures."[8] These are periodic supercells whose lattice sites are occupied by $A$ and $B$ atoms in such a way that the radial correlation functions best match those of the perfectly random *infinite* lattice. Specifically, the SQS-4 structure[8] is used. This supercell is then treated by the same band structure techniques (with the same precision) used to calculate ordinary ordered structures. This method was recently shown[8] to reproduce the band gaps obtained with much larger supercells (containing more than 2000 atoms) whose sites are occupied *randomly* by $A$ and $B$ atoms.

The local density approximation (LDA) is known to systematically underestimate all band gaps.[9] However, this problem can be largely circumvented when we are interested in *relative* changes in band gaps with respect to ordering at a fixed ($x = 1/2$) composition. To do this, we first find the *change* in the relativistically calculated band gap of an ordered structure relative to the calculated average gap of its binary constituents:

$$\delta_{\rm calc} = E_{\rm calc}(ABC_2) - \tfrac{1}{2}[E_{\rm calc}(AC) + E_{\rm calc}(BC)]. \qquad (1)$$

We then obtain the predicted ($p$) gap by applying this change to the average of the *measured*,[10] low-temperature gaps of the constituents

$$E_p(ABC_2) = 1/2[E_{\rm exp}(AC) + E_{\rm exp}(BC)] + \delta_{\rm calc}. \qquad (2)$$

The LDA error largely cancels out when this procedure is applied consistently to each state in $ABC_2$ and to its *corresponding* states in the binary constituents. The overall error in our calculation is estimated to be less than 0.04 eV.

The triply degenerate $\Gamma_{15v}$ valence-band maximum (VBM) is split in the ordered ternary structures into three components both by the noncubic crystal-field (CF) and by spin-orbit (SO) interactions. These splittings reduce the direct band gap. For the $p$-like VBM states, the energies of these three levels can be described well by the quasi-cubic model[11]; relative to their center of gravity, these are

$$E_{1,2,3} = \begin{cases} \tfrac{1}{3}(\Delta_0 + \Delta_{\rm CF}) \\ -\tfrac{1}{6}(\Delta_0 + \Delta_{\rm CF}) \pm \tfrac{1}{2}[(\Delta_0 + \Delta_{\rm CF})^2 - \tfrac{8}{3}\Delta_0\Delta_{\rm CF}]^{1/2} \end{cases} \qquad (3)$$

Here, $\Delta_0$ is the spin-orbit splitting in a cubic field and $\Delta_{\rm CF}$ is the crystal-field splitting (into a singly and a doubly degenerate state in the three order structures) in the absence of spin-orbit interactions. $\Delta_{\rm CF}$ is defined as positive if the doubly degenerate states are above the nondegenerate state. We have fitted our LAPW calculated relativistic VBM energy levels to Eq. (3) and thereby extracted $\Delta_{\rm CF}$ and $\Delta_0$ for the seven systems, given in Table I. For comparison, we also show the values obtained by averaging over the binary constituents. The table shows the following. (i) The difference between $\Delta_0$ for the ordered structures and the value averaged over the binary constituents is small in common-anion systems: $\leqslant 0.01$ eV for III-V systems and $\leqslant 0.04$ eV for II-VI systems (the larger difference in II-VI systems is probably due to the large mixing of d character into the VBM[12]). (ii) The bowing of the spin-orbit splitting can be large and *negative* in common-cation systems.[13] (iii) The crystal-field splitting is small and often negative for CH but generally large and positive in the CA and CP structures (for $GaInP_2$ it is even larger than $\Delta_0$). (iv) By Eq. (3), in structures with negative $\Delta_{\rm CF}$ (e.g., the SQS-4 and some of the CH structures), the upward shift of the top of valence band due to spin-orbit interaction is not $\Delta_0/3$, as commonly assumed by the "$\Delta_0/3$ rule," but rather

$$\delta E = \tfrac{1}{3}\Delta_0 - \tfrac{1}{2}\{\Delta_0 - \Delta_{\rm CF} - [(\Delta_0 + \Delta_{\rm CF})^2 - \tfrac{8}{3}\Delta_0\Delta_{\rm CF}]^{1/2}\}. \qquad (4)$$

However, the simple "$\Delta_0/3$ rule" does apply to the pure binaries as well as to ternary structures with $\Delta_{\rm CF} > 0$.

  

TABLE I. Calculated low-temperature crystal-field splitting $\Delta_{CF}$ and spin-orbit splitting $\Delta_0$ (all in eV) at the VBM for seven 50–50% semiconductor alloys. For comparison, we also give the calculated binary-averaged values. The small LDA correction ( $<0.03$ eV for III-V and $<0.10$ eV for II-VI) for $\Delta_0$ is not included in the binary-averaged value.

| System | Property | Binary average | CA | CH | CP |
|---|---|---|---|---|---|
| $GaInP_2$ | $\Delta_{CF}$ | 0 | 0.191 | 0.032 | 0.212 |
| | $\Delta_0$ | 0.107 | 0.114 | 0.108 | 0.118 |
| $Ga_2AsSb$ | $\Delta_{CF}$ | 0 | 0.085 | −0.013 | 0.230 |
| | $\Delta_0$ | 0.523 | 0.554 | 0.522 | 0.595 |
| $AlGaAs_2$ | $\Delta_{CF}$ | 0 | 0.049 | −0.007 | 0.028 |
| | $\Delta_0$ | 0.319 | 0.317 | 0.319 | 0.320 |
| $ZnCdTe_2$ | $\Delta_{CF}$ | 0 | 0.127 | 0.020 | 0.099 |
| | $\Delta_0$ | 0.873 | 0.864 | 0.868 | 0.854 |
| $ZnHgTe_2$ | $\Delta_{CF}$ | 0 | 0.231 | 0.002 | 0.257 |
| | $\Delta_0$ | 0.831 | 0.831 | 0.828 | 0.793 |
| $CdHgTe_2$ | $\Delta_{CF}$ | 0 | 0.008 | −0.004 | 0.020 |
| | $\Delta_0$ | 0.817 | 0.813 | 0.812 | 0.811 |
| $GaInAs_2$ | $\Delta_{CF}$ | 0 | 0.134 | 0.020 | 0.121 |
| | $\Delta_0$ | 0.351 | 0.355 | 0.352 | 0.347 |

Our calculated direct $\Gamma_{VBM} \rightarrow \Gamma_{1c}$ band gaps (Fig. 1) generally increase in the sequence

$$E_{CP} < E_{CA} < E_R < E_{CH} < \bar{E}, \tag{5}$$

where $\bar{E}$ denotes the 50–50% average of the direct gaps of the binary constituents (the only exceptions are $E_{CH} \gtrsim \bar{E}$ for lattice-matched $AlGaAs_2$ and $CdHgTe_2$). We see that the band-gap narrowing $\delta$ of Eq. (1) is generally small in the chalcopyrite structure but can be very large in the CuPt phase. In fact, *we predict that $\delta_{CP}$ is so large that $AlGaAs_2$ becomes a direct-gap material*[14] *in this structure, despite the fact that the corresponding* 50–50% *random alloy and the CA structure of the alloy have indirect band gaps.* The large variation of the band gaps ( ~0.81 eV for $Ga_2AsSb$) with ordering highlights the possibility of tuning alloy band gaps at a fixed composition by selecting growth conditions[3–6] that favor a particular structure (provided that the samples are uniform). These variations in $E_g$ with ordering could be used as an optical fingerprint to detect particular forms of ordering in a sample. The variation is generally smaller for II-VI systems than for III-V systems. It is interesting to see in Fig. 1 some cases of "band-gap crossings" for different systems in different structures (e.g., $GaInP_2$ has a larger gap than $CdZnTe_2$ both in the chalcopyrite structure and in the random alloy, yet the opposite is predicted to be true in the CuPt structure). Similarly, $CdHgTe_2$ has a smaller gap than $Ga_2AsSb$ in the CH, CA, and random structures, yet in the CuPt structure $Ga_2AsSb$ has a smaller gap than $CdHgTe_2$. A limited number of other calculations for gap narrowing exist in the literature[15–20]; results are quoted in Refs. 15–20 of the present letter.

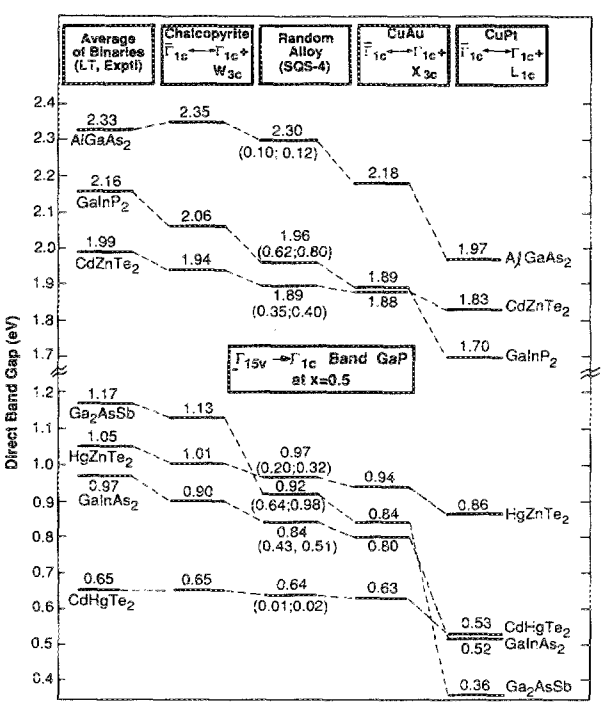


FIG. 1. Predicted low-temperature direct band gaps $\Gamma_{VBM} \rightarrow \Gamma_{1c}$ of seven $ABC_2$ semiconducting systems in the CA, CH, CP, and random (SQS-4) phases. The numbers in the parentheses are bowing coefficients for the random alloy with (first number) or without (second number) crystal-field average, respectively.

The difference between the average band gap and that of the random alloy is $b/4$, where $b$ is the optical bowing coefficient at $x = 1/2$. We give in Fig. 1 our calculated bowing parameters for the random alloy, obtained both with and without averaging over the crystal-field split components of the valence-band maximum in SQS-4. The former values, better representing an isotropic random alloy, compare favorably with the observed[10] bowing parameters.

It is clear from Fig. 1 that ordering-induced changes in the band gap of the pseudobinary $A_{0.5}B_{0.5}C$ alloys far exceed the changes encountered in simple binary polytypes (e.g., zinc blende versus wurtzite). As we noted earlier,[13] these changes can be understood by realizing that these $ABC_2$ ordered compounds are $(AC)_p(BC)_p$ superlattices of repeat period $p$ and orientation $\mathbf{G}$: CuAu is $p = 1$, $\mathbf{G} = [001]$; chalcopyrite is $p = 2$, $\mathbf{G} = [201]$; and CuPt is $p = 1$, $\mathbf{G} = [111]$. Hence, states of different symmetries in the binary constituents can fold into states of identical symmetry in these superlattices. Examples of pairs of zinc-blende states that fold into the $\bar{\Gamma}_{1c}$ superlattice state are given in the heading of Fig. 1; more examples are given in Tables I–III of Ref. 13. This is significant in that isosymmetrical representations can interact and, hence, repel each other by an amount $\Delta E \sim (\Delta V)^2/[\epsilon_i(k) - \epsilon_j(k')]$ that is inversely proportional to their unperturbed energy difference $\epsilon_i(k) - \epsilon_j(k')$ and directly proportional to the square of the coupling matrix $(\Delta V)^2$ (controlled by the potential difference between the $A$ and $B$ atoms and their bond-length mismatch[13]). This repulsion lowers $\bar{\Gamma}_{1c}$ and raises $\bar{\Gamma}_{VBM}$, thus reducing the band gap. Different ordered structures are characterized by different energy denominators and couplings (e.g., in the [111] CuPt structure $L$ folds into $\bar{\Gamma}$, whereas in the [001] CuAu structure $X$ folds into $\bar{\Gamma}$, and in the [201] CH structure $W$ folds into $\bar{\Gamma}$). We can now explain the trends of Fig. 1 in terms of the properties of the binary constituents: (i) The larger band-gap narrowing $\delta_{CP}$ in the CuPt-like structure, relative to $\delta_{CA}$ in the CuAu-like structure, reflects the smaller $\Gamma_{1c}$-

$L_{1c}$ energy denominator (appropriate to CP) relative to the $\Gamma_{1c}$-$X_c$ energy denominator (appropriate to CA). The effect is considerably smaller in CH, where the $\Gamma$-folded $W_c$ states are energetically far removed from $\Gamma_{1c}$, hence the coupling is weaker. (ii) The "band crossings" noted above reflect the same effect: the calculated binary-averaged energy denominator $\Gamma_{1c}$-$L_{1c}$ in GaP-InP ($\sim$0.4 eV) is smaller than that in CdTe-ZnTe($\sim$0.9 eV); hence, $\delta_{CP}$ is larger (0.45 eV) for GaP-InP than for CdTe-ZnTe (0.17 eV). (iii) Among size-matched alloys, $CdHgTe_2$ has a small $\delta_{CP} = 0.12$ eV while $AlGaAs_2$ has a larger $\delta_{CP} = 0.36$ eV, reflecting again a larger energy denominator in the former case (1.3 eV) relative to the latter case (0.4 eV). (iv) $AlGaAs_2$ is predicted to have a larger band-gap narrowing, upon ordering in the CuAu-like structure, than $CdHgTe_2$. This is because the pertinent $\Gamma_{1c}$-$X_{3c}$ energy denominator is larger in the latter case (2.4 eV) than in the former (0.8 eV). (v) The larger crystal-field splitting at the VBM for CA and CP relative to CH (Table I) can also be explained if we notice the larger energy difference $\Gamma_{15v} - W_v$ in CH relative to $\Gamma_{15v} - X_{5v}$ and $\Gamma_{15v} - L_{3v}$ in CA and CP, respectively. (The coupling between $\Gamma$ and $X$ states in CH is very small due to an incompatible phase factor.[13]) (vi) Finally, the stronger $\overline{\Gamma}_4(\Gamma_{15v}) - \overline{\Gamma}_4(W_v)$ coupling relative to the $\overline{\Gamma}_5(\Gamma_{15v}) - \Gamma_5(X_{5v})$ coupling[13] in the chalcopyrite structure can lead to an *inverted* valence band ($\Delta_{CF} < 0$, Table I), whereby the $\Gamma_{4v}$ is *above* the $\Gamma_{5v}$. This is the case in $Ga_2AsSb$, $AlGaAs_2$, and $CdHgTe_2$ (Table I), and also in most real chalcopyrites.[21]

Our calculations compare satisfactorily with the experimental data when nearly perfect monolayer ordering has been achieved experimentally. Ellipsometry measurements[22] of the direct gap of $GaAlAs_2$ in the CA structure gave 2.08 eV at room temperature, or $\sim$2.18 eV when extrapolated to low temperatures. Low-temperature Raman scattering gave[23] 2.15 eV. These values agree well with our prediction (Fig. 1) of 2.18 eV. For $GaInAs_2$ the predicted $\delta_{CA}$-$\delta_{random}$ value of 0.04 eV also agrees well with the experimental value of 0.035 eV of Fukui and Saito.[36] However, the spontaneous ordering achieved to date in most size-mismatched alloys seems to be imperfect; hence, our results (corresponding to an assumed perfect ordering) do not directly apply to currently available samples. Indeed, for metalorgainic chemical vapor deposition grown $GaInP_2$ in the CuPt structure the observed[5,6] $\delta_{CP} \cong 0.21$ eV is much smaller than our value of $\delta_{CP} = 0.46$ eV. Note that currently available samples[5,6] are not only imperfectly ordered but also show *domains* of ordered and disordered phases. We expect that as the degree of ordering and sample uniformity would improve, the measured band gap reductions would approach those of Fig. 1, e.g., $E_g(GaInP_2) \cong 1.70$ eV for CP ordering.

We thank Dr. J. E. Bernard and Dr. A. Mascarenhas for useful discussions. This work was supported by the U.S. Department of Energy under grant No. DE-ACO2-77CH00178.

[1] G. P. Srivastava, J. L. Martins, and A. Zunger, Phys. Rev. B **31**, 2561 (1985); A. Mbaye, L. G. Ferreira, and A. Zunger, Phys. Rev. Lett. **58**, 49 (1987).
[2] L. G. Ferreira, S.-H. Wei, L. G. Ferreira, and A. Zunger, Phys. Rev. B **40**, 3197 (1989); (to be published).
[3] (a) T. S. Kuan, W. I. Wang, and E. L. Wilkie, Appl. Phys. Lett. **51**, 51 (1987); (b) T. Fukui and H. Saito, Jpn. J. Appl. Phys. **23**, L521 (1984).
[4] H. R. Jen, M. J. Cherng, and G. B. Stringfellow, Appl. Phys. Lett. **48**, 1603 (1986).
[5] A. Gomyo, T. Suzuki, A. Kobayashi, S. Kawata, I. Hino, and T. Yuasa, Appl. Phys. Lett. **50**, 673 (1987).
[6] S. R. Kurtz, J. M. Olson, and A. Kibbler, Solar Cells **24**, 307 (1988); T. Nishino, Y. Inoue, and Y. Hamakawa, Appl. Phys. Lett. **53**, 583 (1988).
[7] S.-H. Wei and H. Krakauer, Phys. Rev. Lett. **55**, 1200 (1985).
[8] A. Zunger, S.-H. Wei, L. G. Ferreira and J. E. Bernard (unpublished).
[9] For example, see J. P. Perdew and A. Zunger, Phys. Rev. B **23**, 5048 (1981).
[10] *Landolt-Börnstein New Series*, edited by M. Schulz and H. Weiss (Springer, Berlin, 1982), Vol. 17a,b.
[11] J. J. Hopfield, J. Phys. Chem. Solids **15**, 97 (1960).
[12] S.-H. Wei and A. Zunger, Phys. Rev. B **37**, 8958 (1988).
[13] S.-H. Wei and A. Zunger, Phys. Rev. B **39**, 3279 (1989); **39**, 6279 (1989).
[14] S.-H. Wei and A. Zunger, Appl. Phys. Lett. **53**, 2077 (1988).
[15] D. M. Bylander and L. Kleinman, Phys. Rev. B **34**, 5280 (1986), find $\delta_{CA} = 0.18$ eV in $AlGaAs_2$.
[16] B. J. Min, S. Massidda, and A. J. Freeman, Phys. Rev. B **38**, 1970 (1988), find $\delta_{CA} = 0.18$ eV in $AlGaAs_2$.
[17] P. Boguslawski and A. Baldareschi, Solid State Commun. **70**, 1085 (1989), find $\delta_{CA} = 0.39$ eV in $InGaAs_2$.
[18] A. Taguchi and T. Ohno, Phys. Rev. B **36**, 1696 (1987), find $\delta_{CA} \sim 0$ in $InGaAs_2$.
[19] R. Magri, Phys. Rev. B (to be published) finds $\delta_{CP} = 0.67$ eV in $InGaAs_2$.
[20] T. Kurimoto, N. Hamada, and A. Oshiyama, Superlatt. Microst. **5**, 171 (1989), find $\delta_{CP} = 0.33$ eV in $GaInP_2$.
[21] A. Zunger and J. Jaffe, Phys. Rev. Lett. **51**, 662 (1983).
[22] M. Garriga, M. Cardona, N. E. Christensen, P. Lauten-Schlager, T. Isu, and K. Ploog, Phys. Rev. B **36**, 3254 (1987).
[23] M. Cardona, T. Suemoto, N. E. Christensen, T. Isu, and K. Ploog, Phys. Rev. B **36**, 5906 (1987).